Results in Chemistry 4 (2022) 100443

Contents lists available at ScienceDirect

Results in Chemistry

journal homepage: www.sciencedirect.com/journal/results-in-chemistry

Exploring the chemical space around N-(5-nitrothiazol-2-yl)-1,2,3-thiadiazole-4-carboxamide, a hit compound with serine acetyltransferase (SAT) inhibitory properties

Marialaura Pavone [a], Samanta Raboni [b,e], Marialaura Marchetti [c,d], Giannamaria Annunziato [a], Stefano Bettati [c,d,e], Bianca Papotti [f], Cinzia Marchi [f], Emanuele Carosati [g], Marco Pieroni [a,c,*], Barbara Campanini [b,c], Gabriele Costantino [a,c]

[a] P4T Group and Laboratory of Biochemistry and Molecular Biology, Department of Food and Drug, University of Parma, 43124 Parma, Italy
[b] Laboratory of Biochemistry and Molecular Biology, Department of Food and Drug, University of Parma, 43124 Parma, Italy
[c] Interdepartmental Center Biopharmanet-TEC, University of Parma, Parma 43124, Italy
[d] Department of Medicine and Surgery, University of Parma, Parma 43126, Italy
[e] Institute of Biophysics, National Research Council, Pisa 56124, Italy
[f] Department of Food and Drug, University of Parma, 43124 Parma, Italy
[g] Department of Chemical and Pharmaceutical Sciences, University of Trieste, Trieste 34127, Italy

ARTICLE INFO

Keywords:
Antibiotic adjuvants
Antimicrobial resistance
Non-essential targets
Cysteine biosynthesis
Serine acetyltransferase
Serine acetyltransferase inhibitors

ABSTRACT

The development of the so-called antibiotic adjuvants as inhibitors of non-essential targets represents an innovative and attractive approach to counteract antimicrobial resistance (AMR). Most bacteria rely on the reductive sulfate assimilation pathway (RSAP) to synthesize cysteine, which is a building block for many important biomolecules. Cysteine biosynthetic enzymes are colonization factors that are dispensable during growth in rich media but might become indispensable during host colonization. Being this pathway absent in mammals, it might represent a promising target for drug intervention.

We have focused our attention on compounds targeting serine acetyltransferase (SAT), which is one of the key enzymes involved in the L-cysteine biosynthesis, catalyzing the rate-limiting step of the whole process. In a previous communication, we have reported the discovery through a virtual screening of a new compound (1) with promising SAT inhibitory activity. The capability of this compound to interfere with bacterial growth in the cell assays prompted us to carry out a medicinal chemistry campaign to further investigate its potential. We herein report the synthesis of compound 1 analogues to define the structure–activity relationships (SAR) of this series of potential SAT inhibitors regarding the target binding and general toxicity. Despite the improvement in the inhibitory activity of some molecules, the toxicity profile needs to be fine-tuned, and these findings will be used to drive the synthesis of new analogues.

1. Introduction

The World Health Organization (WHO) has included antimicrobial resistance (AMR) in the top 10 major urgent threats to human health [1]. AMR is a natural phenomenon that occurs when bacteria, viruses, fungi, and parasites acquire or develop the ability to survive when exposed to antimicrobials [2]. If no urgent action is taken, the number of people who will die due to AMR will increase to 10 million each year by 2050 [3].

Currently, years of oblivion in the search of novel antibacterials have led to a poor pipeline, and to face the increasing number of multi-drug resistant (MDR) bacterial strains, the discovery of new treatments has become as relevant as ever before [4,5]. Besides the "classical" discovery approaches, new strategies may encompass the development of new antibiotic adjuvants [6], which are chemical entities characterized by weak or absent antibiotic activity but that, when co-administrated with antibiotics, may boost their efficacy against susceptible and resistant bacterial strains [7]. Since these drugs are not supposed to inhibit any crucial cellular function of the bacteria, another advantage would be the reduction of the selective pressure that leads to the development of

* Corresponding author at: P4T Group, Department of Food and Drug, University of Parma, 43124 Parma, Italy.
E-mail address: marco.pieroni@unipr.it (M. Pieroni).

https://doi.org/10.1016/j.rechem.2022.100443
Received 11 April 2022; Accepted 14 July 2022
Available online 18 July 2022

resistance [8–10]. Therefore, the administration of such molecules with existing antibiotics may result in a winning strategy to prevent the raise of resistances and safeguard the current antibacterial arsenal. In this regard, strong evidence has proved that suppression or reduction of cysteine biosynthesis lead to a decrease of bacterial fitness and a reduction of virulence [11–18]. Most bacteria spend part of their life-cycle in harsh conditions and challenging environments, like macrophages or gastric mucosa. In these conditions, interfering with any of the pathogen adaptation systems may reduce their virulence and persistence and, as a consequence, increase susceptibility to antibiotics [19]. Cysteine is essential to all organisms, and many investigations, e.g. in *Salmonella*, *Vibrio fischeri* and *Mycobacterium tuberculosis*, have highlighted its pivotal role in processes that are relevant to infection such as biofilm formation, response to oxidative stress and persistence [20]. For instance, it has been demonstrated that in mutants lacking cysteine biosynthesic pathway in *Salmonella enterica* serovar Typhimurium, due to the inactivation of cysteine biosynthesis, unpaired oxidative stress can lead to a decrease in antibiotic resistance in both vegetative and swarm cell populations [15].

Cysteine biosynthesis is carried out by the reductive sulfate assimilation pathway (RSAP), which is absent in mammals [21]. The RSAP begins with the active transport of sulfate, the principal source of sulfur present in the environment, inside the cell. Once in the cell, sulfate undergoes a multi-step reduction to bisulfite, which is eventually incorporated into cysteine *via* a β-elimination reaction on *O*-acetylserine (OAS) catalyzed by *O*-acetylserine sulfhydrylase (OASS, encoded by *cysK*). OAS is formed by the action of the preceding enzyme in the pathway, serine acetyltransferase (SAT, encoded by *cysE*). SAT catalyzes the rate-limiting step of cysteine biosynthesis, in which an acetyl group from acetyl-CoA (AcCoA) is transferred to the hydroxyl of L-serine to generate OAS, a molecule with a better leaving group. Under sulfur limitation OAS accumulates and spontaneously converts to *N*-acetylserine (NAS), the natural inducer of cysteine regulon [22]. Noteworthy, inhibition of SAT might concurrently block cysteine biosynthesis and the expression of the genes involved in sulfate transport and reduction. From the structural point of view, SAT is a dimer of trimers, with an α-helical *N*-terminal domain and a terminal left-handed β-helix domain ending with a flexible, disordered C-terminal sequence that binds OASS at the active site, and it is responsible for its competitive, partial inhibition [23–28].

We have recently spent efforts in the design and synthesis of molecules able to inhibit both OASS and SAT. Different approaches, from the ligand-based drug design to the target-based virtual screening of chemical libraries, were carried out [14,29–31]. In the case of OASS, these efforts culminated in the most potent inhibitor of OASS known so far, (1S,2S)-1-(4-methylbenzyl)-2-phenylcyclopropane-1-carboxylic acid, namely **UPAR415** (Fig. 1), with a K_D in a low nanomolar range [32,33].

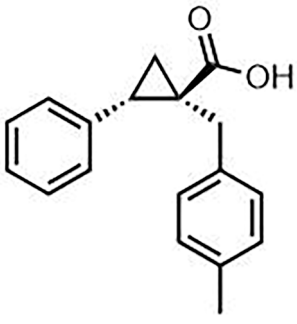

UPAR415

Fig. 1. Chemical Structure of **UPAR415**.

Despite its remarkable affinity towards the enzyme, **UPAR415** failed to show good activity in bacterial cells, likely for the lack of sufficient cellular penetrability. Therefore, after exploring OASS as a pharmaceutical target, we moved our focus to the search of new SAT inhibitors that, differently from OASS inhibitors which lead to OAS accumulation, are expected to cause both cysteine and OAS depletion. To our knowledge, only a few attempts to discover potential SAT inhibitors are reported in the literature [34,35]. In this regard, we have recently reported the identification of a series of isoxazoles derivatives as a promising class of SAT inhibitors through drug repurposing. The synthesis of new 2-aminooxazole analogues successfully led to molecules with IC_{50} values between 1 and 11 μM. Despite the promising inhibitory activity, even the most active compounds could not interfere with bacterial growth [36]. Also in this case, the scarce ability of penetrating the bacterial cell wall might be accounted for the lack of cellular activity.

Another virtual screening was performed using commercial Chemdiv focused anti-infective, antifungals, and antiviral/antibacterial libraries, containing 91,243 compounds, that allowed us to discover compound **1** (Fig. 2A) as a new promising inhibitor of SAT with an encouraging activity toward SAT from *Salmonella enterica* serovar Typhimurium (*St*SAT) ($IC_{50} = 48 \pm 6$ μM). Moreover, compound **1** was found to have a MIC of 64 μg/ml in minimal medium, while it does not show any antibacterial activity in rich medium, a solid suggestion that the specific inhibition of cysteine biosynthesis is responsible for the phenotype, as we have previously reported [37].

These preliminary results, coupled with the synthetic accessibility of analogues, prompted us to further explore the chemical space around compound **1**, with the aim to identify new derivatives with improved affinity for the target and define the structure–activity relationships (SAR). This synthetic studies were complemented with a preliminary docking analysis, that helped to partially rationalize the SAR information collected.

2. Results and discussion

2.1. Chemistry

The final compounds were obtained through standard amide coupling reaction, starting from the appropriate amine and the carboxylic acids, suitably activated with 1,1′-carbonyldiimidazole (CDI) (Scheme 1). When the desired compounds could not be obtained *via* this method, *O*-(Benzotriazol-1-yl)-*N,N,N′,N′*-tetramethyluronium tetrafluoroborate (TBTU) and *N*-(3-Dimethylaminopropyl)-*N′*-ethylcarbodiimide hydrochloride (EDC•HCl) were used as the coupling agents, whereas the conversion of the acids to the corresponding acyl chlorides and the subsequent reaction with the 2-amino-5-chlorothiazole allowed the isolation of **62** and **63**, even if in a low yield, likely due to the poor reactivity of the 2-amino-5-chlorothiazole.

The majority of the carboxylic acids were commercially available, or in some cases, the methyl esters were purchased and then hydrolyzed. Thiophene derivatives with an aromatic substituent at C-4 and benzothiophene with an aromatic substituent at C-6 were synthesized *via* Suzuki-Miyaura cross-coupling reaction using XPhos Pd G2 as a catalyst (Scheme 2).

All the amines used were purchased, except for the 2-amino-5-phenylthiazole (**70V**), synthesized in two steps starting from phenylacetaldehyde, which was first alpha-brominated, and then reacted with thiourea according to the Hantzsch protocol (Scheme 3).

Compound **30** was synthesized via an addition reaction between the 2-amino-5-nitrothiazole and an appropriate isocyanate under an inert atmosphere, using triethylamine as the base and toluene as solvent. Nevertheless, as reported in Scheme 4, a different protocol was used to obtain urea **29** and its derivatives **27** and **28**. 2-amino-5-nitrothiazole was first reacted with phenyl chloroformate to obtain the carbamate derivative **26**, which was irradiated in a microwave reactor with the proper aliphatic amine. This procedure proved to be a versatile, rapid,

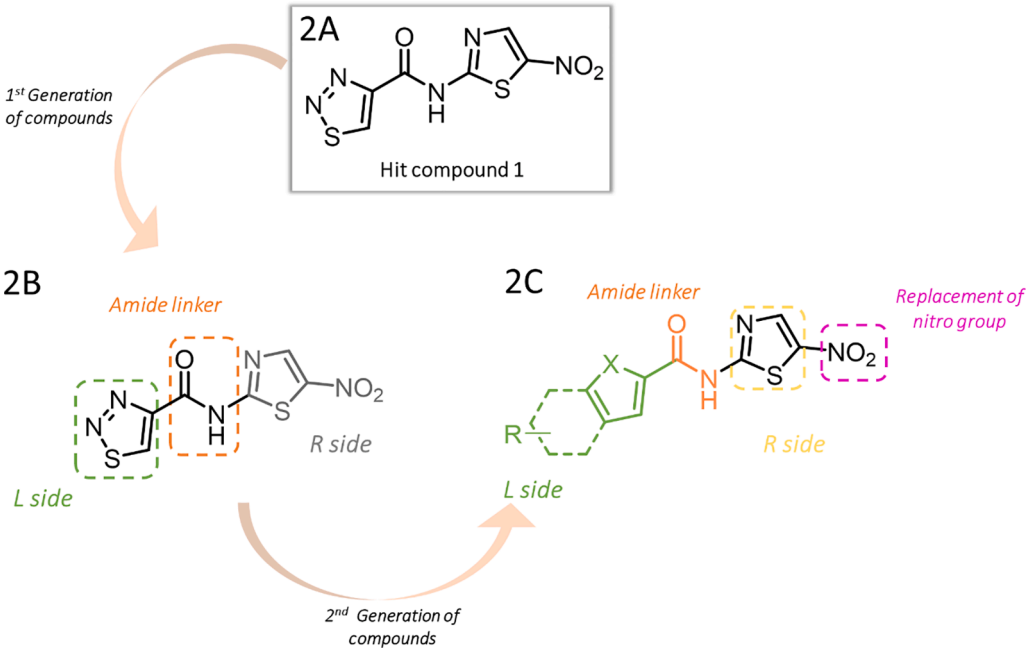

Fig. 2. Hit compound modifications. **2A**) Hit compound **1**. **2B**) Modifications led to the 1st generation of compounds; **2C**) Modifications explored during the second round of optimization and leading to the 2nd generation of compounds.

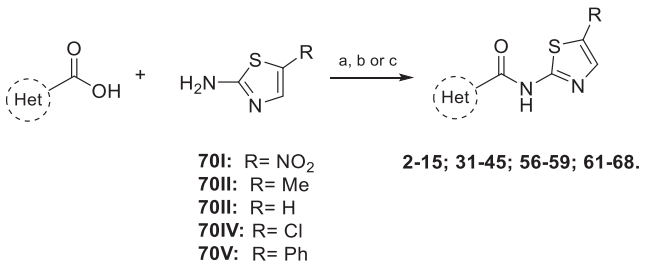

Scheme 1. [a] Reagents and conditions: a) TBTU, EDC, DIPEA, DMAP, DMF dry, rt, 67–5 %; b) CDI, DMF dry, rt, on; c) 1) $(COCl)_2$, DMF dry, DCM dry, N_2 atm, rt, 4 h; 2) Pyridine, DCM dry, 50 °C, 15 h, 12 %. [b] For complete structures, see Table 1 and Table 2.

and efficient protocol to obtain a variety of urea derivatives starting from the most common reagents [38]. The chemical structures of the synthesized compounds were confirmed on the basis of their NMR and mass spectra.

2.2. Structure-activity relationships (SAR)

Compound **1** is structurally characterized by two small heterocycles, a thiadiazole and a 2-aminothiazole ring, linked through an amide bond. We deemed it was worthwhile to modify each part of the hit structure, introducing different groups to evaluate the contribution of each portion of the molecule to the overall activity. During the first round of investigation, the 2-amino-5-nitrothiazole moiety was kept intact, and modifications to the linker and substitutions of the thiadiazole were carried out. In the second generation of compounds, hints from the SAR were used to substitute the nitro group attached to the 2-aminothiazole with other small functional groups (Fig. 2**B**).

The lead compound optimization started with the synthesis of a small

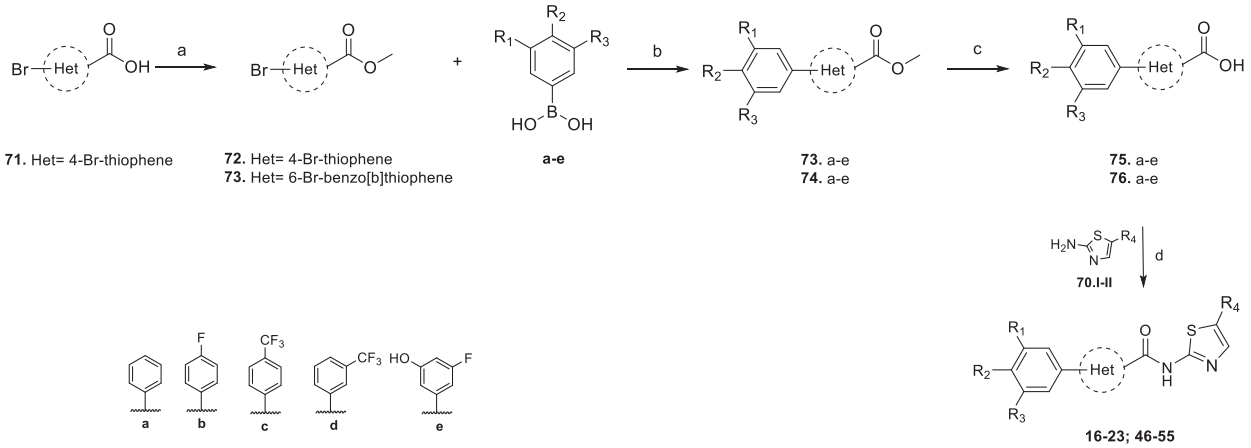

Scheme 2. [a]Reagents and conditions: a) CH_3I, K_2CO_3, DMF, rt, 15 h, 70%; b) 1) K_3PO_4, THF/H_2O, N_2 atm, 10 min, 2) XPHOS PdG2, 70 °C, 90 min, 93–47%; c) LiOH in THF/H_2O/MeOH 3:1:1, r.t, 1–5 h, 100–74%; d) 1) CDI, DMF dry, N_2 atm, rt, 1 h, 2) amine, 70 °C, on, 71–12%. [b]For complete structures, see Table 1 and Table 2.

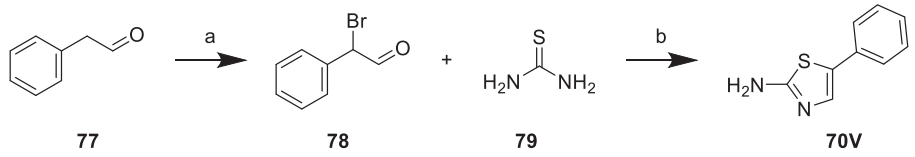

Scheme 3. [a]Reagents and conditions: a) Br_2, DCM, r.t; b) EtOH, reflux, on, 20%.

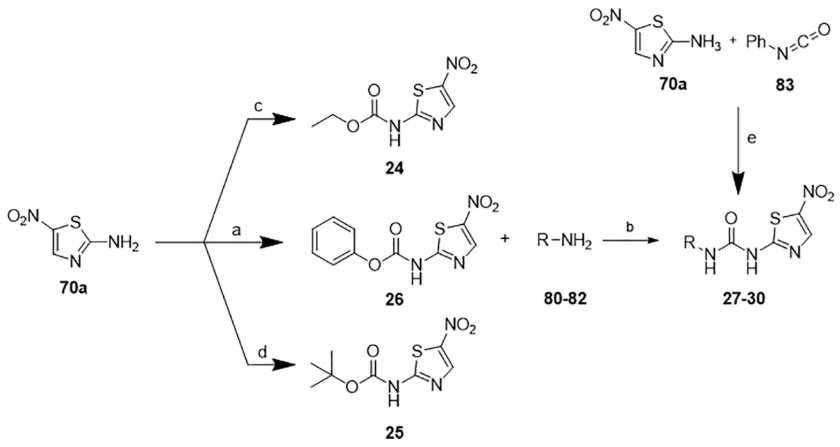

Amine	R
80	i-Pr
81	c-Pr
82	H

Scheme 4. [a]Reagents and conditions: a) Phenyl chloroformate, pyridine, DCM dry, 90 min, rt; 86%; b) THF dry, MW (T: 150 °C, Power: 300W, Time: 20 min, Pressure: 250 PSI); 80–10%; c) Ethyl chloroformiate, THF dry, 66 °C, 2 h; 31%; d) Boc_2O, DMAP, Et_3N, THF dry, r.t, 4.5h; 58%; Et_3N, DCM dry, 0 °C- r.t, 15 h; 33%.

set of compound **1** derivatives in order to collect preliminary information about the SAR in relation to their IC_{50} (Table 1).

At first, the thiadiazole ring was substituted with five-membered heterocycles, like thiazole (**2**), pyrrole (**3**), and oxazole (**4**). Surprisingly, no one of these compounds had an inhibitory activity equal to or greater than the hit compound **1** (**2**, **3**, **4**, $IC_{50} > 100$ μM). Subsequently, phenyl and 2-pyridine were used as the substituent, but also in this case, no improvement in the activity could be detected (**5**, **6**, $IC_{50} > 100$ μM). At this point, bulkier steric bicycles were investigated as substituents of the thiadiazole group. In this case, the replacement of the thiadiazole with a group such as benzo[*b*]thiophene, 4,5,6,7-tetrahydrobenzo[*b*]thiophene, indole, and benzimidazole led to an appreciable activity (**7**, $IC_{50} = 18 \pm 2$ μM; **8**, $IC_{50} \cong 63$ μM; **9**, $IC_{50} = 23 \pm 1$ μM; **10**, $IC_{50} \cong 43$ μM) with the exception of the benzotriazole ring (**11**, $IC_{50} > 100$ μM).

Taking advantage from the fact that these heterocyclic structures could be further modified, we deemed of interest to explore the activity of substituted benzothiophene analogues.

In this regard, a set of derivates bearing various small functional groups was synthesized. Electron withdrawing groups (EWGs), such as chlorine and fluorine, and an electron donor group (EDG), such as the methyl, were introduced at positions C-3 and C-6 of the scaffold (**12**–**15**). All the substituents introduced to the benzo[*b*]thiophene ring were well tolerated, with some of them (**13**, **14**) noticeably improving the affinity of the molecule for the enzyme (**12**, $IC_{50} = 28 \pm 4$ μM; **13**, $IC_{50} = 10 \pm 1$ μM; **14**, $IC_{50} = 5.2 \pm 0.5$ μM). The EDG at the C-6 was the only exception, being compound **15** ($IC_{50} > 100$ μM) the only derivative with a weaker activity compared to compound **1**. After exploring the impact of derivatives bearing small functional groups, we also investigated the effect of bulkier substituents to obtain molecules with enhanced steric hindrance, which was achieved by adding phenyl substituents at the C-6 of the moiety *via* Suzuki coupling (**16**–**19**). Introducing *m*-fluorophenol moiety at the C-6 led to a derivative with a considerable increase in inhibitory activity (**16**, $IC_{50} = 1.5 \pm 0.2$ μM). On the contrary, the compound bearing the *p*-CF_3-phenyl ring showed a slight decrease in the activity (**17**, $IC_{50} = 66 \pm 20$ μM). Additionally, a noteworthy inhibitory activity was also detected when *p*-fluorophenyl and phenyl rings were used as substituents at the C-6 of the benzo[*b*]thiophene moiety (**18**, $IC_{50} \cong 4$ μM; **19**, $IC_{50} \cong 5$ μM). Subsequently, to reduce the rigidity of the structure although preserving its hindrance, the benzo[*b*]thiophene core was replaced with a thiophene bearing substituted phenyl rings at the C-4 (**20**–**23**). As for the benzo[*b*]thiophene derivatives, the presence of *m*-fluorophenyl moiety led to a compound with higher inhibitory activity (**20**, $IC_{50} = 6 \pm 1$ μM). On the other hand, substituents as the *p*-CF_3 and the *m*-CF_3 phenyl were able to confer a similar inhibitory potency (**21**, $IC_{50} = 28 \pm 4$ μM; **22**, $IC_{50} \cong 12$ μM). Apparently, it could be speculated that five-membered heterocycles are tolerated as long as their hindrance is augmented by the addition of a bulky substituent.

From this first round of modifications, we concluded that the thiadiazole ring could be effectively replaced with other heterocycles, with a particular predilection for sulfurated heterocycles such as benzothiophene and substituted thiophene rings.

In a similar vein, we also synthesized a small set of derivatives where the amide linker between the 2-amino-5-nitrothiazole and the thiadiazole was substituted by two different structural bridges, namely the carbamate and the urea. All of these molecules showed low potency and a strong absorption at 412 nm. Because the activity assay relies on the signal of TNB at 412 nm, for most inhibitors only a limited concentration range could be tested in order to maintain the absorbance value below 2 OD. For this reason, for these molecules only an approximated IC_{50} value could be determined (**24**, **25**, **27**, **28**, $IC_{50} > 100$ μM; **26**, $IC_{50} \cong 80$ μM; **29**, $IC_{50} = 101 \pm 9$ μM, **30**, $IC_{50} = 107 \pm 14$ μM). Therefore, the investigation of these modifications was suspended.

The nitro group, which possesses a strong EWG nature, has been often associated with toxicity issues, and for this reason, it is usually considered a structural alert in the design of molecules [39]. Considering this, we wanted to evaluate the toxicity of those derivatives with the most encouraging inhibitory activity (**1**, **7**–**9**, **12**–**14**, **16**–**23**). Unfortunately, all of the molecules tested were found to be toxic, including those ranked as the best compounds, namely **14**, **16**, **18**, **19**, and **20**. This information pushed us to start another round of modification to try to couple a good inhibitory potency with a favorable toxic profile.

First, we deemed of interest to replace the 2-amino-5-nitrothiazole moiety with other heterocycles and explore the impact on the activity.

Table 1
*St*SAT Inhibitory activity (IC_{50}) and cytotoxicity toward THP-1 cells (CC_{50}) of 1st Generation of compounds.

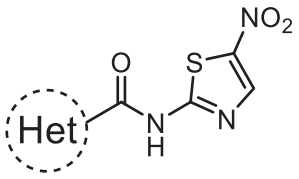

Cpd	Het	IC_{50} (μM)	Cytotoxicity CC_{50} (μM)	Cpd	Het	IC_{50} (μM)	Cytotoxicity CC_{50} (μM)
1		48±6	< 25	**16**	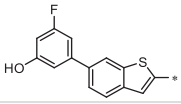	1.5 ± 0.2	< 25
2		> 100	N/A	**17**	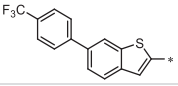	66 ± 20	< 25
3		> 100	N/A	**18**	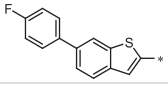	≅4*	< 25
4		> 100	N/A	**19**	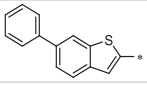	≅5*	< 25
5		> 100	N/A	**20**	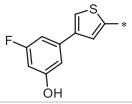	6.1 ± 1.2	< 25
6		>100	N/A	**21**	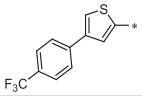	28 ± 4	< 25
7		18 ± 2	<25	**22**	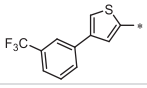	≅12*	< 25
8		63*	<25	**23**	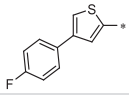	≅57*	<25
9		23 ± 1	<25	**24**		>100	N/A
10		≅43*	N/A	**25**		>100	N/A
11		>100	N/A	**26**		≅80*	N/A
12		28 ± 4	< 25	**27**		>100	N/A
13	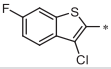	10 ± 1	< 25	**28**		>100	N/A
14	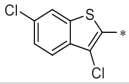	5.2 ± 0.5	< 25	**29**		101 ± 9	N/A
15	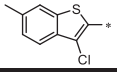	> 100	< 25	**30**		107 ± 14	N/A

* low-solubility compounds. The IC_{50} was calculated in a limited concentration range (usually highest tested concentration lower than or equal to IC_{50}), and for this reason, only an estimate is given.

N/A: not available

Then, the 2-aminothiazole core was retained, although having at position 5 substituents other than the nitro group (Table 2).

Concerning the first attempt, compounds **31** and **32** were prepared. The thiazole ring was integrated into a steric and bulky moiety to increase the structural rigidity to the *R*-side of the molecule and evaluate the biological effect of a higher-character π-system. The 2-aminothiazole was condensed to pyridine and phenyl to give 2-aminobenzothiazole and 2-aminopyridothiazole derivatives. Although modified, the aminothiazole ring was maintained in this case, though no improvement in the inhibitory activity could be detected (**31**, **32**, $IC_{50} > 100$ μM). In a different setting, the thiazole moiety was substituted with pyridine, but, also in this case, the modification proved to be detrimental (**33**, **34**, $IC_{50} > 100$ μM). This also applied when the thiadiazole was substituted with an indole, which in the previous series (**9**) proved to be efficacious (**35**, **36**, $IC_{50} > 100$ μM).

Since the substitution of the 2-amino-5-nitrothiazole with different bulky substituents did not bring any improvement to our purpose, we started to investigate the substitution of the nitro moiety with other functional groups such as hydrogen, chlorine, and phenyl.

For these compounds, first, the thiadiazole ring was connected to the 2-aminothiazole, without any functional groups at C-5, through an amide linker to evaluate how this substitution affected the activity (**38**). Then, the thiadiazole was substituted with those heterocycles that, in the 1st round of modifications, were able to confer good activity. Removal of the nitro group led to a loss of activity when the 2-aminothiazole is linked to the thiadiazole. Furthermore, replacing the thiadiazole ring with a bulky group on the *L*-side of the molecule did not prove beneficial for the enzymatic activity (**38**, **39**, $IC_{50} > 100$ μM).

Substitution with the methyl, which is a lipophilic group but with different electronic characteristics compared to the nitro, did not improve the activity compared to the parent compound (**40**, $IC_{50} > 100$ μM; **1**, $IC_{50} = 48.6 \pm 8.43$ μM). However, this compound did not show appreciable toxicity, with a $CC_{50} > 200$ μM, which was remarkably higher than that of **1** ($CC_{50} < 25$ μM). Encouraged by the lack of toxicity, we decided to repeat some of the substitutions used for modifying compounds **1** to **40**. This led to a series of compounds (**41**–**59**) with a wide range of biological properties that can be summarized as follows. Regarding the benzo[*b*]thiophene derivatives, the unsubstituted compound, or the substitution with a methyl group at C-3 or an F at C-6 and Cl at C-3, showed a drop in the inhibitory activity compared to the nitro analogues (**41**, $IC_{50} > 100$ μM; **7**, $IC_{50} = 18 \pm 2$ μM; **42**, $IC_{50} > 100$ μM; **12**, $IC_{50} = 28 \pm 4$ μM; **43**, $IC_{50} > 100$ μM; **13**, $IC_{50} = 10 \pm 1$ μM). On the other hand, Cl at C-6 and C-3 led to a methyl derivate with a very good inhibitory activity comparable to that of the nitro-derivative, although the toxicity profile was still inadequate (**44**, $IC_{50} = 13 \pm 4$ μM, $CC_{50} < 25$ μM; **14**, $IC_{50} = 5.2 \pm 0.5$ μM,). Surprisingly, the removal of Cl at C-6 brings a derivative with an enhanced toxic profile and only a small decrease in the inhibitory activity (**45**, $IC_{50} = 65 \pm 9$ μM; $CC_{50} > 200$ μM). The pattern with a 6-phenylbenzo[*b*]thiophene moiety and a 2-amino-5-methylthiazole (**46**–**50**) seems to be advantageous to the inhibitory activity. Unexpectedly, the only modification leading to a detrimental effect for the inhibitory activity was that represented by the *m*-fluorophenol moiety as a substituent at C-6, a group that led to one of the most active compounds in the nitro series. Despite these encouraging preliminary results, the introduction of the methyl group on the thiazole ring did not significantly improve the toxicity profile of these derivatives. Surprisingly, **46**, bearing a *p*-CF_3-phenyl moiety at the C-6, was the only exception that led to a derivate that showed higher cellular viability in the MTT assay, although the activity was concentration-independent in the range from 10 nM to 25 μM (Table 2). Furthermore, the decoration with substituted phenyl moieties led to only partial inhibition of the enzymatic activity even at the highest concentrations tested, pointing to solubility issues.

With regard to the thiophene derivatives, compounds **51**–**53**, and **55** showed inhibitory activity of <100 μM. Compound **51** was the only phenylthiophene derivate that led to remarkable cellular viability, coupled with an appreciable IC_{50} (**51**, $IC_{50} \cong 15$ μM, $CC_{50} > 200$; **52**, $IC_{50} \cong 77$ μM, $CC_{50} < 25$; **53**, $IC_{50} \cong 50$ μM, $CC_{50} < 25$; **54**, $IC_{50} > 100$ μM, $CC_{50} < 25$; **55**, $IC_{50} \cong 27$ μM).

Among the other bulky substituents used for the 2-amino-5-methylthiazole derivates, only the indole moiety showed a comparable activity towards the enzyme to compound **1**, allowing low cellular viability (**56**, $IC_{50} \cong 43$ μM, $CC_{50} < 25$; **57**, $IC_{50} > 100$ μM; **58**, $IC_{50} = 70 \pm 9$ μM; **59**, $IC_{50} > 100$ μM). Concerning the *N*-methylation of the indole, this modification did not lead to any improvement to the activity compared with the *N*-unsubstituted analogue (**60**, $IC_{50} = 53 \pm 1$ μM; **56**, $IC_{50} \cong 43$ μM).

As mentioned above, the most active compound in the nitro series showed a drop in the activity when a methyl substituent was added (**47**, $IC_{50} > 100$ μM; **16**, $IC_{50} = 1.5 \pm 0.2$). On the contrary, other compounds in the methyl series have kept an inhibitory activity<100 μM, even if higher compared to the nitro analogue (i.e, **14**, $IC_{50} = 5.2 \pm 0.5$; **44**, $IC_{50} = 13 \pm 4$; **21**, $IC_{50} = 28 \pm 4$; **53**, $IC_{50} \cong 50$; **20**, $IC_{50} = 6.1 \pm 1.2$; **55**, $IC_{50} \cong 27$). Therefore, the SAR related to the nitro derivatives cannot be applied also to the methyl derivatives.

Replacing the nitro group with Cl, an EWD, or a group such as a phenyl was found to be a suitable solution for the inhibitory proprieties of the molecule. When the nitro was substituted with the chlorine group, a similar behavior could be noticed as for the methyl substitution. Indeed, the substitution with the thiadiazole led to a derivative with scarce potency (**61**, $IC_{50} > 100$ μM), whereas the substitution with bulky heterocycles groups led to appreciable-affinity compounds (**62**, $IC_{50} = 22 \pm 3$ μM; **63**, $IC_{50} = 19$ μM). Unfortunately, the high toxicity of these molecules discouraged the study of further derivatives.

Differently, replacing the nitro with the phenyl moiety, and linking it to the thiadiazole ring, led to a compound with an inhibitory activity < 100 μM (**64**, $IC_{50} \cong 67$ μM). This may serve as preliminary speculation that also bulky substituent attached to the 2-aminothiazole could improve the activity towards SAT. The inhibitory activity was lost when the phenyl moiety was introduced at the C-4 of the 2-aminothiazole (**65**, $IC_{50} > 100$ μM). The replacement of the thiadiazole moiety with bulky groups, such as indole, benzo[*b*]thiophene, and 3,6-dichlorobenzo[*b*]thiophene, still led to compounds with a good activity towards the enzyme. However, as for the chlorine derivates, these derivatives resulted in being toxic, the only exception being represented by compound **66**, which showed an improvement in the cytotoxicity profile (**66**, $IC_{50} = 17 \pm 5$ μM, $CC_{50} = 87.73$; **67**, $IC_{50} = 25 \pm 6$ μM; $CC_{50} = 33.76$; **68**, $IC_{50} = 4.8 \pm 0.9$ μM, $CC_{50} < 25$). Further investigation will follow to understand whether indole derivatives linked to the 2-amino-5-phenylthiazole ring could allow higher cellular viability.

3. Chemical space exploration via structure-activity landscape and molecular docking analysis

Nowadays, the structure–activity landscape can be easily navigated through open-source chemoinformatics tools; [40,41] we explored the chemical space by means of a similarity map, created with the software Data Warrior [42]. The location in the map of each compound is determined by its structure similarity versus the other molecules of the dataset, with connections limited to pairs of similar compounds (Fig. 3). On the resulting map, molecules are colored by activity (indicated as pIC_{50}), whereas their size is given by the corresponding SALI (Structure-Activity Landscape Index) scores, a metrics that numerically reports how much activity is gained (or lost) accordingly to structural changes [43]. For each pair of molecules with measured activity *a1* and *a2* and structural similarity being *s*, the score is calculated as $SALI = |a1\text{-}a2| / (1\text{-}s)$. A molecule with three connections in the map will have three SALI scores, with the mean value used to assign its size. Molecule pairs with high SALI score represent information-rich structural motifs, and their comparative study might help in the understanding of SAR. The analysis of the dataset of SAT inhibitors is reported in Fig. 3, where a set of (green-to-yellow) inactive satellites surround three groups of molecules

Table 2
*St*SAT Inhibitory activity (IC_{50}) and cytotoxicity toward THP-1 cells (CC_{50}) of 2*nd* Generation of compounds.

Cpd	Structure	IC_{50} (μM)	Cytotoxicity CC_{50} (μM)	Cpd	Structure	IC_{50} (μM)	Cytotoxicity CC_{50} (μM)
31	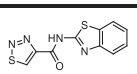	>100	N/A	**50**	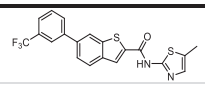	≅ 18*	N/A
32	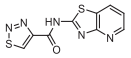	>100	N/A	**51**	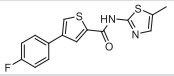	≅ 15*	>200
33	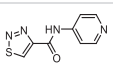	> 100	N/A	**52**	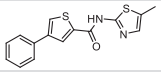	≅ 77*	<25
34	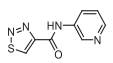	> 100	N/A	**53**	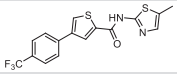	≅ 50*	<25
35	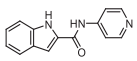	>100	N/A	**54**	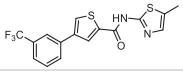	>100	<25
36	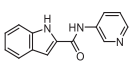	> 100	N/A	**55**	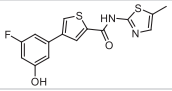	≅ 27*	N/A
37	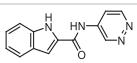	> 100	N/A	**56**	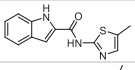	≅ 43*	<25
38	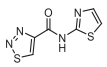	> 100	N/A	**57**	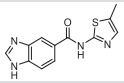	>100	N/A
39	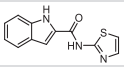	>100	N/A	**58**	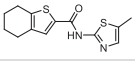	70 ± 9	N/A
40	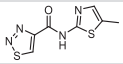	>100	>200	**59**	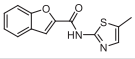	>100	N/A
41	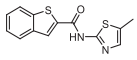	>100	N/A	**60**	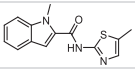	53 ± 1	N/A
42	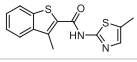	>100	N/A	**61**	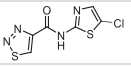	>100	N/A
43	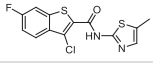	> 100	N/A	**62**	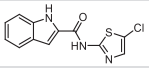	22 ± 3	26.3
44	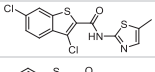	13±4	<25	**63**	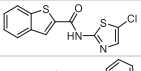	19*	<25
45	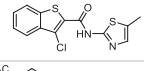	65 ± 9	>200	**64**	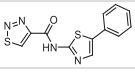	67*	<25
46	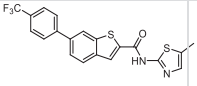	N.D.**	144.5	**65**	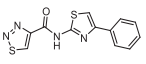	>100	N/A
47	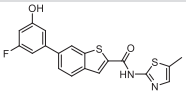	> 100	<25	**66**	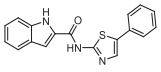	17±5	87.73
48	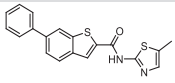	≅ 14*	<25	**67**	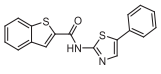	25 ± 6	33.76
49	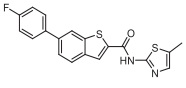	≅ 42*	39.76	**68**	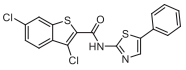	4.8 ± 0.9	<25

* low-solubility compounds. The IC_{50} was calculated in a limited concentration range (usually highest tested concentration lower than or equal to IC_{50}), and for this reason, only an estimate is given.

** the activity was concentration-independent in the range 10 nM and 25 μM.

N/A: not available

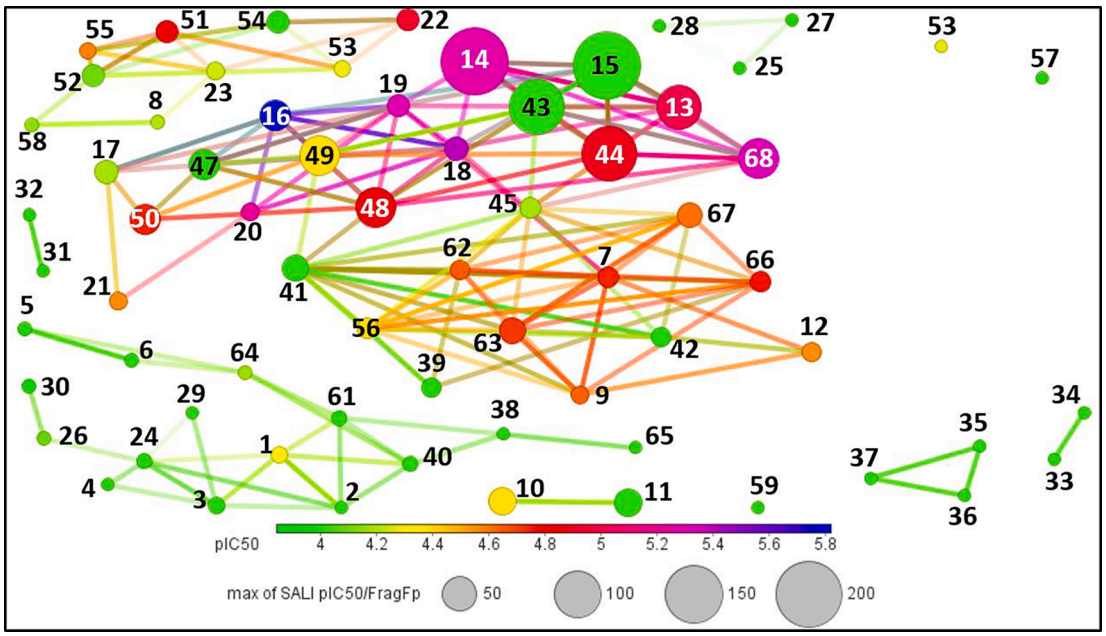

Fig. 3. Scaffold clustering of the SAT inhibitors. Molecules were described with the FragFP method (a fragment-based description), followed by an optimization procedure (based on the Rubberbanding forcefield) to equilibrate the relative (neighboring) position of similar molecules. Molecules are coloured by pIC_{50} values from green (inactive) to blue (strong activity). Only similar molecules are connected (those pairs with similarity over a threshold value, set to 95%), whereas the size of the spots is given by the Structure-Activity Landscape Index (SALI) score (the larger the size, the larger the activity cliff). (For interpretation of the references to colour in this figure legend, the reader is referred to the web version of this article.)

connected each other by several links, as described below. The first group, on the left-side upper corner of the plot, is composed by three active molecules (**22**, **51** and **55**), and some molecules with medium-to-low (**8**, **23** and **53**) or very low, if any, inhibitory activity (**52**, **54** and **58**). This set of molecules have comparable low SALI scores, meaning that variations on inhibitory activity are paired to structural variations.

Molecules part of the cluster in the middle of the plot are characterized by different heterocycles on the *L*-side; this group contains molecules with a broad activity range (17–100) but comparable low SALI scores; as already discussed, information-rich SAR can arise by comparing active molecules (**7**, **9**, **12**, **62**, **63**, **66** and **67**) to molecules with low (**45** and **56**) or no (**39**, **41**, **42**) activity.

Finally, between the two mentioned clusters there is the largest group of molecules, composed of 16 diverse derivatives, from the most potent of the series (**13**, **14**, **16**, **18**, **19**, **20**, **21**, **44**, **48**, **50** and **68**) to a few of medium-to-low activity (**17**, **49**) or even inactives (**15**, **43** and **47**). This large cluster is composed of non-homogeneous structures, with large substituents as well as small substituents on both sides (L and R).

Among this cluster we observed interesting activity-cliffs, i.e. pairs of structurally similar active compounds with a large difference in potency [44]. An example of activity cliff is the pair of compounds **14** *vs* **15**, where a drop in activity is observed when substituting a chlorine atom with a methyl group.

Docking studies are often used to identify the key structural features of the ligands and to formulate hypotheses to understand the protein–ligand interactions. Therefore, a molecular docking study was carried out to further investigate what emerged from the Structure-Activity Relationships (section 2.2) and from the Structure-Activity Landscape analysis. At the time of writing, the entry 1T3D [45,46] was the only crystal structure of SAT for *E.coli* available in the protein data bank; [46] a preliminary analysis of the 3D structure and the binding sites allowed to identify the cysteine site as potential binding pocket for the series of SAT inhibitors presented herein.

The software AutoDock Vina [47,48] was used on a binding pocket centered on the ligand CYS501, with a cubic grid with box size set to 20 Å and spacing set to 0.375 Å. Docking experiments were carried out for the molecules of the three mentioned groups, the solutions were sorted by the lowest affinity scores and visualized with AutoDockTools [AutodockTools, version 1.5.7] and PyMol [W.L. DeLano. The PyMOL Molecular Graphics System, DeLano Scientific LLC, CA, Palo Alto (2008)].

Fig. 4 reports the binding site with either the cysteine (4A) or all the docked molecules (4B), with one docking solution (pose) per compound.

A comparative analysis along the dataset, including the three best poses for each molecule, led to the identification of a few poses outside the cysteine binding site and a set of common molecular orientations. A detailed analysis of all the binding modes for all the studied compounds is out of the scope of the present paper; here, guided by the SALI analysis, we report in Fig. 5 a representative set of molecules from the three groups, in order to identify the key interactons for the most active SAT inhibitors. Noteworthy, the majority of active molecules share common binding modes, whereas docking solutions for the inactive ones often do not share the same modes (with steric hindrance being the most likely cause).

The key interactions of the active molecules involve the following residues and groups: the NH_2 of Asn-134, often involved in hydrogen bonding interaction with the nitro group; the COO^- of Asp-157, involved in the interaction with the NH of amide linker; the NH_2 of Gln-258, involved in medium or weak hydrogen bonds with OH, F or CF_3 substituents of the phenyl ring; a protonated NH of the imidazole ring of His-193, involved in hydrogen bonding interactions with the O from the carbonyl group of the amide linker; a neutral N nitrogen of the imidazole ring of His-158 and the O from the carbonyl group of Mse-256, both involved in halogen bonds with substituents of the benzothiophene ring.

These observations can help explaining some of the activity cliffs observed; for example, the detrimental replacement of the nitro with methyl, or the detrimental replacement of the a chlorine with a methyl in the benzothiophene ring. In some other cases, cause-effect relationship of chemical modification cannot be inferred from docking results due to different size and shape of the molecule that cause a different orientation in the binding site.

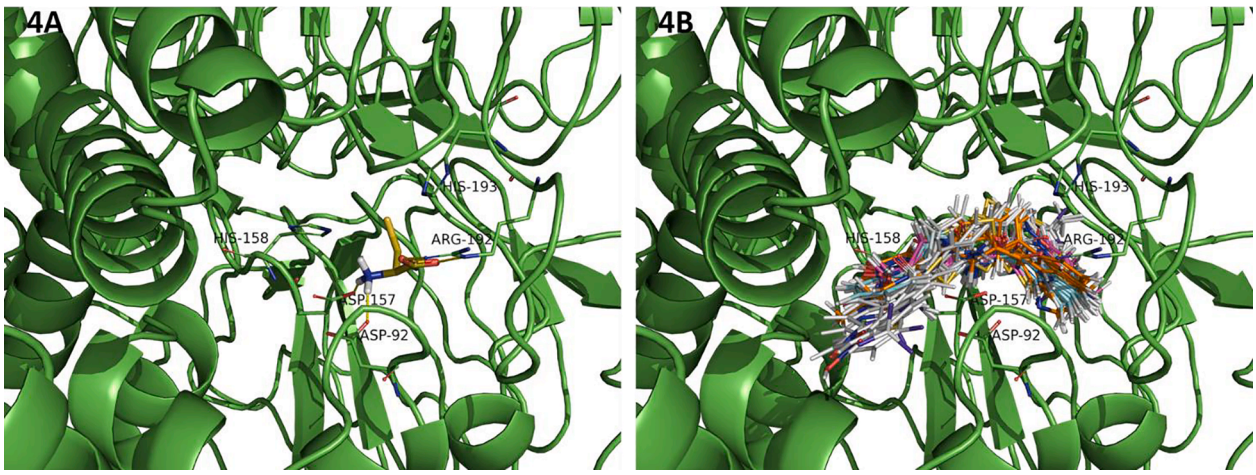

Fig. 4. Binding site of the Cysteine of the PDB entry 1T3D (4A) and docking results for a set of SAT inhibitors, coloured according to the groups from the similarity map analysis (4B). The key residues are labeled: the amino group of cysteine interacts with two carboxylic groups of Asp-192 and Asp-157, whereas its carboxylic group interacts with Arg-92; two histidines (His-158 and His-193) create a favourable location for the SH group.

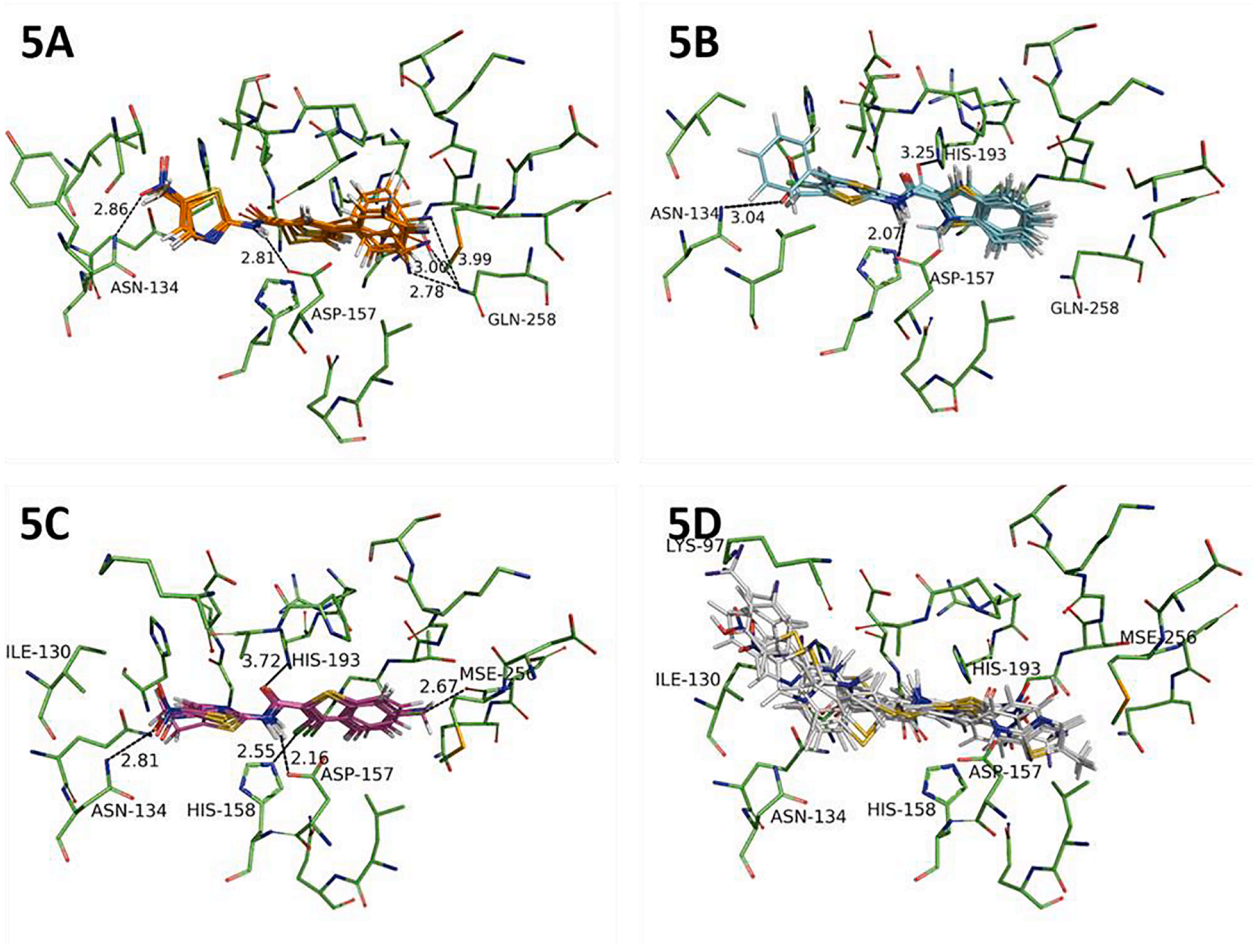

Fig. 5. Docking solutions for subset of SAT inhibitors. A) Compounds **22**, **23**, **51**, **52** and **55** (all active). B) Compounds **7**, **9**, **12**, **45**, **56**, **62**, **63**, **66** and **67** (all active). C) Compounds **13**, **14**, **44**, **45** (active) as well as **15** and **43** (inactive). D) Compounds **16**, **18**, **19**, **20**, **21**, **48**, **50** (all active).

4. Conclusion

The discovery of hit compound **1** as a promising SAT inhibitor prompted us to carry out a medicinal chemistry campaign to obtain molecules with improved biological properties. Two generations of compounds were synthesized and analyzed to define a preliminary SAR, considering both enzymatic inhibition and toxicity to THP-1 derived macrophages cells.

In general, introducing bulky groups in the *L*-side of the molecules demonstrated to be particularly advantageous for the inhibitory effect of the molecules. Nevertheless, besides the good inhibitory activity shown by some compounds, all those bearing EWGs such as nitro or chlorine at

the C-5 of the 2-aminothiazole showed high toxicity in MTT assay, even at a concentration of 25 μM. As for the *L*-side of the molecule, the introduction of bulky lipophilic substituents, like the phenyl at the C-5 of the 2-aminothiazole, on the other side, appears beneficial regarding the inhibitory activity. This information might lead to further explore the hindrance of the thiadiazole ring to improve the toxic profile of the molecule. Indeed, the indole moiety linked to the 2-amino-5-phenylthiazole (**66**) showed a better cytotoxic profile than the corresponding analogue with a benzo[*b*]thiophene core. Compounds with 2-amino-5-methylthiazole have shown borderline results, and, surprisingly, the most active compounds within the nitro series resulted inactive when the methyl is used in place of the NO_2 moiety at C-5. Furthermore, unlike **40**, that showed an excellent cytotoxicity profile, most of these derivates are toxic in the assays used. Only three compounds belonging to the methyl derivatives showed an acceptable toxicity profile (**45**, **46**, **51**) coupled to good inhibitory activity, resulting in the most promising compounds derived from this investigation. From these SAR data, it might be speculated that the combination of the methyl group at the C-5 of the thiazole and appropriate halogen groups on the benzo[*b*]thiophene or 4-phenylthiophene ring in the *L*-side of the molecule led to compounds with improved cytotoxicity profiles, and as for compound **51**, also an inhibitory activity 3-fold increase compared to the hit compound (**45**, $IC_{50} = 65 \pm 9$ μM, $CC_{50} > 200$ μM; **46**, $CC_{50} = 144.5$; **51**, $IC_{50} \cong 15$ μM, $CC_{50} > 200$). The data above described were also analyzed with the help of computational methods. A small set of derivatives were docked in the enzyme binding pocket and important preliminary information could be collected. In particular, some of the key interactions of the molecules with the enzyme were sustained by the NO_2 group, somehow justifying the absence of activity for the majority of molecules lacking this functional group. However, these studies might set the stage for the rationale synthesis of improved analogues. Considering the few SAT inhibitors reported in the literature and the growing interest in the research of potent inhibitors of such enzyme, the progress achieved in this work and the bulk of information collected might be exploited for the design and synthesis of drug-like SAT inhibitors, as it is currently ongoing in our lab.

5. Materials and methods

5.1. Chemistry

All the reagents were purchased from Sigma-Aldrich, Alfa-Aesar, and Fluorchem at reagent purity and, unless otherwise noted, were used without any further purification. Dry solvents used in the reactions were obtained by distillation of technical grade materials over appropriate dehydrating agents. Reactions were monitored by thin-layer chromatography on silica gel-coated aluminum foils (silica gel on Al foils, SUPELCO Analytical, Sigma-Aldrich) at 254 and 365 nm. MCRs were conducted using CEM CEM Discover Synthesis Unit (CEM Corp., Matthews, NC). Where indicated, intermediates and final products were purified through silica gel flash column chromatography (silica gel, 0.040–0.063 mm) or Combiflash® Rf 200, using appropriate solvent mixtures. ^{1}H NMR and ^{13}C NMR spectra were recorded on a BRUKER AVANCE spectrometer (^{1}H at 300 or 400 MHz and ^{13}C at 75 or 101 MHz respectively) or a JEOL spectrometer (^{1}H at 600 MHz and ^{13}C at 125 MHz), with TMS as an internal standard. ^{1}H NMR spectra are reported in this order: δ ppm (multiplicity, number of protons). Standard abbreviations indicating the multiplicity were used as follows: s = singlet, d = doublet, dd = doublet of doublets, t = triplet, q = quadruplet, m = multiplet, and b = broad signal. Low-resolution mass spectrometry measurements were performed on quattromicro API tandem mass spectrometer (Waters, Milford, MA, USA) equipped with an external APCI or ESI ion source. ESI-mass spectra are reported in the form of (*m/z*).

General procedure for the amidation reaction

Method A: *O*-(Benzotriazol-1-yl)-*N,N,N′,N′*-tetramethyluronium tetrafluoroborate (TBTU) (1.00 eq) and *N*-(3-dimethylaminopropyl)-*N′*-ethylcarbodiimide hydrochloride (EDC·HCl) (1.00 eq) were added to a solution of the proper carboxylic acid (1 eq) in dry DMF (4 mL/mmol) under nitrogen atmosphere. The reaction mixture was stirred at room temperature for 15 min, then triethylamine (1.5 eq) and the amine (1.00 eq) were added. The mixture was stirred at the same temperature for 4–12 h. Then, the reaction mixture was extracted with EtOAc (3x10 mL), the organic layers were collected, washed with brine (2x10 mL), and dried over Na_2SO_4. After filtration, the volatiles were removed under vacuum, and the crude material was purified by flash column chromatography eluting with DCM/MeOH. Purification conditions, yields, and analytical data are reported in the supporting information.

Method B: Carbonyldiimidazole (CDI) (1.00 eq) was added to a solution of the proper carboxylic acid (1.00 eq) in dry DMF (2 mL/mmol) under N_2 atmosphere. The reaction mixture was left stirring for 1 h at room temperature, and then the amine (1.00 eq) was added. The reaction mixture was heated to 70 °C overnight. The reaction was quenched with water and extracted with EtOAc (3x10 mL). The organic layers were dried over anhydrous Na_2SO_4, filtered, and concentrated under reduced pressure. The crude was purified by flash column chromatography eluting with DCM/MeOH or with trituration. Purification conditions, yields, and analytical data are reported in the supporting information.

Method C: The proper carboxylic acid (1.00 eq) was suspended in anhydrous DCM (6 mL/mmol), and anhydrous DMF (0.06 mL/mmol) under N_2 atmosphere, and then oxalyl chloride (2 M solution in DCM, 2 eq) was added slowly to the stirred suspension. The reaction mixture was stirred at room temperature for 2 h. After this time, the solvent was evaporated under reduced pressure. The crude was re-dissolved in anhydrous DCM (5 mL/mmol). A suspension of 2-amino-5-chlorothiazole (1.00 eq) and pyridine (1.00 eq) in anhydrous DCM (1.2 mL/mmol) was added dropwise, and the reaction mixture was stirred at 50 °C overnight. The reaction was cooled to room temperature, and water was added and extracted with EtOAc (3x10 mL). Organic layers were collected, dried over anhydrous Na_2SO_4, filtered, and concentrated under reduced pressure. The crude was purified by flash column chromatography (DCM/MeOH) to give the title compounds. Purification conditions, yields, and analytical data are reported in the supporting information.

Ethyl (5-nitrothiazol-2-yl)carbamate (24): 2-amino-5-nitrothiazole (**70I**) (250 mg, 1.72 mmol) was dissolved in THF, and then ethyl chloroformate (202 mg, 1.86 mmol) was added. The reaction mixture was refluxed overnight. The solvent was evaporated under reduced pressure, and the crude was purified by flash column chromatography (petroleum ether/EtOAc from 85:15 to 80:20) to give the title compound as a white powder (yield: 31%). ^{1}H NMR (400 MHz, DMSO-d_6): δ 12.85 (s, 1H); 8.56 (s, 1H); 4.29 (q, $J = 7.1$ Hz, 2H); 1.29 (t, $J = 7.1$ Hz, 3H). ^{13}C NMR (100.6 MHz, $CDCL_3$): δ 164.6; 152.9; 143.3; 140.1; 63.9; 14.4. HPLC-ESI-MS analysis: calculated for $C_6H_7N_3O_4S$: 217.02; found: 218.07 [M+H$^+$].

***Tert*-butyl (5-nitrothiazol-2-yl)carbamate (25):** 2-amino-5-nitrothiazole (**70I**) (500 mg, 3.44 mmol), DMAP (3.43 mg, 0,028 mmol), di-*tert*-butyl dicarbonate (826 mg, 3.78 mmol), TEA (0.16 mL/mmol) were suspended in anhydrous THF (0.5 mL/mmol). The reaction mixture was stirred at room temperature overnight. Then, DCM was added, and the reaction mixture was washed with HCl 0.1 N, and water. The organic layer was dried over anhydrous Na_2SO_4, filtered, and concentrated under reduced pressure. The crude was purified by flash column chromatography (Petroleum Ether/EtOAc 7:3) to give the title compound as an orange powder (yield: 58 %). ^{1}H NMR (400 MHz, DMSO-d_6): δ 12.58 (bs, 1H); 8.53 (s, 1H); 1.56 (s, 9H). ^{13}C NMR (100.6 MHz, $CDCL_3$): δ 164.8; 153.2; 143.8; 142.1; 83.7; 28.2. HR-MS analysis: calculated for $C_8H_{11}N_3O_4S$: 245.01; found: 246.11 [M + H +].

Phenyl (5-nitrothiazol-2-yl)carbamate (26): 2-amino-5-nitrothiazole (**70I**) (400 mg, 2.76 mmol) and pyridine (0.267 mL, 3.31 mmol) were dissolved in anhydrous DCM (1 mL/mmol), and then phenyl

chloroformate (518 mg, 3.31 mmol) was added dropwise under N_2 atmosphere at 0 °C. The reaction mixture was stirred at room temperature for 90 min.

After the consumption of starting material, water was added to the reaction mixture, and it was extracted with EtOAc (3x10 mL). Organic layers were collected, dried over anhydrous Na_2SO_4, filtered, and concentrated under reduced pressure. The crude was purified by flash column chromatography (Petroleum ether/EtOAc 8:2) to give the title compound as a yellow powder (yield: 52%). ^{1}H NMR (400 MHz, DMSO-d_6): δ 13.41 (s, 1H); 8.63 (s, 1H); 7.48–7-0.46 (m, 2H); 7.34–7.31 (m, 3H). ^{13}C NMR (100.6 MHz, DMSO-d_6): δ 164.6; 153.1; 150.3; 143.6; 142.8; 130.2; 126.9; 122.1. HR-MS analysis: calculated for $C_{10}H_7N_3O_4S$: 265.01; found: 266.11 [M+H$^+$].

General procedure for the synthesis of urea derivatives

Method A: In a microwave tube, carbamate **26** (1.00 eq) and the proper aliphatic amine (1.5 eq) were dissolved in THF, and the reaction mixture was heated in a microwave reactor with the following parameters: 150 °C, 25 min, 300 W, 250 psi, power max: off. At the end of the irradiation, water was added to the reaction mixture, and it was extracted with EtOAc (3x10 mL). The crude was purified by flash column chromatography (DCM/MeOH) to give the title compounds. Purification conditions, yields, and analytical data are reported in the supporting information.

Method B: To a cold solution (0 °C) of phenyl isocyanate (82 mg, 0.69 mmol) in anhydrous DCM (2.90 mL/mmol) under N_2 atmosphere were added 5-nitro-aminothiazole (100 mg, 0.69 mmol) and TEA (0.287 mL, 2.07 mmol). The reaction mixture was stirred at room temperature. After the complete consumption of the starting material, the reaction was poured into ice, and water was added. The aqueous phase was extracted with DCM (3x10 mL), and the organic layers were dried over anhydrous Na_2SO_4, filtered, and concentrated under reduced pressure. The crude material was purified by flash column chromatography. Purification conditions, yields, and analytical data are reported in the supporting information.

General procedure for the Suzuki-Miyaura Cross-Coupling reaction

To a solution of methyl 4-bromothiophene-2-carboxylate (**72**) or methyl 6-bromobenzo[*b*]thiophene-2-carboxylate (**73**) (1.00 eq) in THF/H_2O (3:1, 10 mL/mmol) were added the appropriate boronic acid or ester (1.5 eq) and potassium phosphate tribasic (2.00 eq). The mixture was stirred under a nitrogen atmosphere for 10 min. After this time, X-Phos Pd G2 (0.15 eq) was added, and the reaction mixture was stirred at 70 °C for 2 h. After cooling to room temperature, the reaction mixture was filtered through a plug of Celite. The filtrate was concentrated under reduced pressure, and the residue was extracted with EtOAc (3x10 mL), dried over anhydrous Na_2SO_4, filtered, and concentrated under reduced pressure. The crude was purified by flash column chromatography eluting with Petroleum Ether/EtOAc. Purification conditions, yields, and analytical data are reported in the supporting information.

General procedure for the hydrolysis of the carboxylic esters

LiOH (4.00 eq) was added to a solution of the proper carboxylic ester (1.00 eq) in THF/MeOH/H_2O (3:1:1), and the reaction mixture was stirred at room temperature for 2 h. 1N HCl was added to the mixture until acid pH. When a precipitate occurs, it was filtered off. Otherwise, the mixture was extracted with EtOAc (3x10 mL), and the organic layers were dried over anhydrous Na_2SO_4, filtered, and concentrated under reduced pressure. The product was used in the next step without further purification. Yields and analytical data are reported in the supporting information.

5-Phenylthiazol-2-amine (70V): To a solution of phenylacetaldehyde (2.0 g, 16.65 mmol) in DCM (1 mL/mmol), a solution of Br_2 (0.854 mL, 16.65 mmol) in DCM (0.6 mL/mmol) was added dropwise. After consumption of the starting material according to TLC, the solvent was removed in vacuo, having care not to heat the bath >20 °C, to prevent the evaporation of the brominated compound. Without further purification, the red crude oil obtained was quickly reacted with thiourea (2.38 g, 31.32 mmol) in absolute ethanol (1 mL/mmol) at reflux overnight. The mix was recrystallized with 30% MeOH in water to obtain the title compound as a pale-yellow powder (yield: 20%). ^{1}H NMR (400 MHz, DMSO-d_6): δ 7.42–7-39 (m, 3H); 7.33 (t, J = 7.6 Hz, 2H); 7.20–7.16 (m, 1H); 7.13 (s, 2H). HR-MS analysis: calculated for $C_9H_8N_2S$: 176.04; found: 177.21 [M + H$^+$].

Methyl 4-bromothiophene-2-carboxylate (72): A mixture of 4-bromothiophe-2-carboxylic acid (500 mg, 2.42 mmol), K_2CO_3 (700 mg, 5.07 mmol), and CH_3I (0.451 mL, 1.25 mmol) in DMF (2 mL/mmol) was stirred at room temperature overnight. Water was added to the reaction mixture, and it was extracted with EtOAc (3x10 mL). The organic layers were dried over anhydrous Na_2SO_4, filtered, and concentrated under reduced pressure. The product was used in the next step without further purification (yield: 70%). ^{1}H NMR (400 MHz, $CDCL_3$): δ 7.71 (s, 1H); 7.47 (s, 1H); 3.20 (s, 3H).

5.2. Activity assays

*St*SAT was expressed recombinantly in *E. coli* using published methods [37]. The gene coding for StSAT was inserted in pSH21p-His6-trxA plasmid (a kind gift from Professor Christopher S. Hayes, MCDB, University of California, Santa Barbara). The expression was carried out in *E. coli* Tuner™ BL21(DE3) cells (Novagen, Merck Biosciences, Billerica, MA, USA) in LB added of 150 μg/mL ampicillin and 1% glucose. Cells were grown at 37 °C and induced with 1 mM IPTG for 4 h. The protein was purified in 100 mM Tris buffer added of 500 mM NaCl, 50 μM L-cysteine, 1 mM TCEP, pH 7.5 by affinity chromatography on Talon™ resin (Takara Bio, Shiga, Japan). Endogenous *O*-acetylserine sulfhydrylase bound to *St*SAT was eluted with 10 mM OAS. *St*SAT was eluted with imidazole and the His6-trxA tag was cleaved by in-house produced TEV protease that was eventually removed by size exclusion chromatography using HiLoad 16/600 Superdex 75 prep grade column. The final enzyme preparation was >95% pure based on the SDS-PAGE analysis. Activity assays were carried out following the method published in Magalhães *et al.*, [37] with some modifications. Briefly, the enzyme activity was measured by a spectrophotometric indirect continuous assay that exploits the signal at 412 nm generated by 5,5′-Dithiobis(2-nitrobenzoic acid DTNB - Ellman's reagent) reduction by the reaction product coenzyme A. The assay is carried out at 20 °C in a cuvette-format using a Cary 4000 UV–vis spectrophotometer (Agilent, Santa Clara, CA, USA) equipped with a cuvette holder thermostated through a circulating water bath. The buffer was 20 mM sodium phosphate, 85 mM NaCl, 1 mM EDTA, 5% DMSO, 1 mM DTNB, 1 mM L-Ser and 0.25 mM acetyl-CoA, pH 7.0. The concentration of *St*SAT was 70 nM. The reaction was initiated by addition of acetyl-CoA to the reaction mixture. The compounds were first screened at a fixed 100 μM concentration. Only those compounds showing a residual activity lower than 50% were subjected to further assays to calculate the IC_{50} values. The dependence of the relative reaction rate on the concentration of compounds was fitted to the equation to calculate the IC_{50}:

$$\frac{v_i}{v_0} = \frac{1}{1 + \frac{[I]}{IC_{50}}}$$

Compounds bearing a nitro group, i.e. all the first generation compounds, strongly absorb at 412 nm, thus making the determination of the inhibitory activity problematic. The use of 3 mm-pathlength cuvettes allowed to mitigate the issue, but in some cases the range of inhibitor concentrations tested was limited. Some of the compounds, especially those with the thiadiazole ring substituted by larger and more hydrophobic groups, showed low solubility in the assay buffer at pH 7.0. For these compounds, only data at low compound concentrations ($\leq IC_{50}$) were used for the fitting, and this affected the accuracy of the estimated IC_{50}. For this reason, the IC_{50} values of these inhibitors are given as an estimate ($\cong$) without the error.

5.3. Cytotoxicity assay and CC_{50} determination. Cell culture.

Human monocytes THP-I cells were grown in suspension in RPMI 1640 (Euroclone, Italy) supplemented with 1% Sodium Pyruvate 100 mM (Life Technologies, USA), 0.5% Gentamicin 10 mg/ml (Sigma Aldrich, USA), 0.1% 2-Mercaptoethanol 50 mM (Life Technologies, USA), Glucose (0,25 g/ml) and 10% Fetal Bovine Serum (FBS; Euroclone, Italy). THP-I cells were kept at 37 °C and 5% CO_2 in a sterile incubator for all the experimental procedures described.

THP-1 cells were seeded in 24-well plates (Sarstedt, Germany), with a density of 500,000 cells/well in the presence of 100 ng/mL of phorbol 12-myristate 13-acetate (PMA; Sigma-Aldrich, USA) for 72 h to allow the cells to differentiate into macrophages.

5.4. Cytotoxicity assay (MTT assay).

MTT assay has been used to assess the cytotoxicity of synthesized compounds in THP-derived macrophages by evaluating the ability of mitochondrial succinate dehydrogenase to catalyze the enzymatic reduction of yellow water-soluble 3-[4,5-dimethylthiazole-2-yl]-2,5-diphenyltetrazolium bromide (MTT; Sigma Aldrich, USA) to insoluble purple formazan, index of cell viability. Differentiated macrophages were treated with synthesized compounds at increasing concentrations (25 μM, 50 μM, 100 μM, and 200 μM; all compounds were tested as a triplicate) for 72 h. 20 mM compounds solutions in DMSO were prepared, and consequentially diluted to obtain a final concentration up to 200 μM, corresponding to 1% v/v of DMSO. Control cells were treated with the same amount of DMSO (1% v/v), to subtract the cell damage induced by DMSO from that specifically induced by the analyzed compounds. Afterwards, control and compound-treated cells were incubated with a solution of 1 mg/ml of MTT dissolved in RPMI 1640, supplemented with 5% FBS, at 37 °C, 5 % CO_2 for 2 h in dark. The solution was then removed, and resulting formazan crystals were dissolved in 0.2 mL DMSO under shaking for 10 min. Finally, absorbance was measured on an aliquot of 0.15 mL at a wavelength of 570 nm using an absorbance microplate reader (Spark® Tecan, Switzerland) [49]. CC_{50} of each compound was then calculated by interpolating the mean value of the tested concentrations from the dose–response curve as compared to the control cells, whose viability was considered as 100%.

CRediT authorship contribution statement

Marialaura Pavone: Data curation, Writing – original draft. **Samanta Raboni:** Data curation, Writing – original draft. **Marialaura Marchetti:** Data curation, Writing – original draft. **Giannamaria Annunziato:** Data curation, Writing – original draft. **Stefano Bettati:** Visualization, Investigation. **Bianca Papotti:** Data curation, Writing – original draft. **Cinzia Marchi:** Data curation, Writing – original draft. **Emanuele Carosati:** In silico modeling. **Marco Pieroni:** Conceptualization, Methodology, Supervision, Writing – review & editing. **Barbara Campanini:** Visualization, Investigation, Supervision. **Gabriele Costantino:** Visualization, Investigation, Supervision, Writing – review & editing.

Declaration of Competing Interest

The authors declare that they have no known competing financial interests or personal relationships that could have appeared to influence the work reported in this paper.

Aknowledgements

This work was funded under the MSCA-ITN-2014-ETN project INTEGRATE [grant number 642620]. Acknowledgments: The Centro Interdipartimentale Misure “G. Casnati” is kindly acknowledged for the contribution in the analytical determination of the molecules synthesised.

References

[1] Ten threats to global health in 2019. https://www.who.int/news-room/spotlight/ten-threats-to-global-health-in-2019.
[2] Antimicrobial resistance. Accessed November 30, 2021. https://www.who.int/news-room/fact-sheets/detail/antimicrobial-resistance.
[3] ANTIMICROBIAL RESISTANCE Global Report on Surveillance.
[4] E. Charani, M. McKee, R. Ahmad, M. Balasegaram, C. Bonaconsa, G.B. Merrett, R. Busse, V. Carter, E. Castro-Sanchez, B.D. Franklin, P. Georgiou, K. Hill-Cawthorne, W. Hope, Y. Imanaka, A. Kambugu, A.JM. Leather, O. Mbamalu, M. McLeod, M. Mendelson, M. Mpundu, T.M. Rawson, W. Ricciardi, J. Rodriguez-Manzano, S. Singh, C. Tsioutis, C. Uchea, N. Zhu, A.H. Holmes, Optimising antimicrobial use in humans – review of current evidence and an interdisciplinary consensus on key priorities for research, Lancet Reg. Health - Europe 7 (2021) 100161.
[5] K.M.G. O'Connell, J.T. Hodgkinson, H.F. Sore, M. Welch, G.P.C. Salmond, D. R. Spring, Combating multidrug-resistant bacteria: Current strategies for the discovery of novel antibacterials, Angew. Chem. – Internat. Ed. 52 (41) (2013) 10706–10733, https://doi.org/10.1002/anie.201209979.
[6] G. Annunziato, Strategies to overcome antimicrobial resistance (AMR) making use of non-essential target inhibitors: A review, Int. J. Mol. Sci. 20 (23) (2019), https://doi.org/10.3390/ijms20235844.
[7] Y. Liu, R. Li, X. Xiao, Z. Wang, Antibiotic adjuvants: an alternative approach to overcome multi-drug resistant Gram-negative bacteria, Crit. Rev. Microbiol. 45 (3) (2019) 301–314, https://doi.org/10.1080/1040841X.2019.1599813.
[8] C. Baron, Antivirulence drugs to target bacterial secretion systems, Curr. Opin. Microbiol. 13 (1) (2010) 100–105, https://doi.org/10.1016/j.mib.2009.12.003.
[9] A.E. Clatworthy, E. Pierson, D.T. Hung, Targeting virulence: A new paradigm for antimicrobial therapy, Nat. Chem. Biol. 3 (9) (2007) 541–548, https://doi.org/10.1038/nchembio.2007.24.
[10] D.A. Rasko, V. Sperandio, Anti-virulence strategies to combat bacteria-mediated disease, Nat. Rev. Drug Discovery 9 (2) (2010) 117–128, https://doi.org/10.1038/nrd3013.
[11] F. Spyrakis, P. Felici, A.S. Bayden, E. Salsi, R. Miggiano, G.E. Kellogg, P. Cozzini, P. F. Cook, A. Mozzarelli, B. Campanini, Fine tuning of the active site modulates specificity in the interaction of O-acetylserine sulfhydrylase isozymes with serine acetyltransferase, Biochim. Biophys. Acta - Proteins Proteomics. 1834 (1) (2013) 169–181.
[12] F. Spyrakis, R. Singh, P. Cozzini, B. Campanini, E. Salsi, P. Felici, S. Raboni, P. Benedetti, G. Cruciani, G.E. Kellogg, P.F. Cook, A. Mozzarelli, B.G. Vertessy, Isozyme-specific ligands for O-acetylserine sulfhydrylase, a Novel Antibiotic Target, PLoS ONE 8 (10) (2013) e77558.
[13] M. Marchetti, F.S. De Angelis, G. Annunziato, G. Costantino, M. Pieroni, L. Ronda, A. Mozzarelli, B. Campanini, S. Cannistraro, A.R. Bizzarri, S. Bettati, A competitive o-acetylserine sulfhydrylase inhibitor modulates the formation of cysteine synthase complex, Catalysts. 11 (6) (2021) 700.
[14] G. Annunziato, M. Pieroni, R. Benoni, B. Campanini, T.A. Pertinhez, C. Pecchini, A. Bruno, J. Magalhães, S. Bettati, N. Franko, A. Mozzarelli, G. Costantino, Cyclopropane-1,2-dicarboxylic acids as new tools for the biophysical investigation of O-acetylserine sulfhydrylases by fluorimetric methods and saturation transfer difference (STD) NMR, J. Enzyme Inhib. Med. Chem. 31 (sup4) (2016) 78–87.
[15] A.L. Tumbull, M.G. Surette, L-Cysteine is required for induced antibiotic resistance in actively swarming Salmonella enterica serovar Typhimurium, Microbiology 154 (11) (2008) 3410–3419, https://doi.org/10.1099/mic.0.2008/020347-0.
[16] A.L. Turnbull, M.G. Surette, Cysteine biosynthesis, oxidative stress and antibiotic resistance in Salmonella typhimurium, Res. Microbiol. 161 (8) (2010) 643–650, https://doi.org/10.1016/j.resmic.2010.06.004.
[17] M.J. Wallace, S. Dharuman, D.M. Fernando, S.M. Reeve, C.T. Gee, J. Yao, E. C. Griffith, G.A. Phelps, W.C. Wright, J.M. Elmore, R.B. Lee, T. Chen, R.E. Lee, Discovery and characterization of the antimetabolite action of thioacetamide-linked 1,2,3-triazoles as disruptors of cysteine biosynthesis in gram-negative bacteria, ACS Infect. Dis. 6 (3) (2020) 467–478.
[18] P.B. Palde, A. Bhaskar, L.E. Pedró Rosa, F. Madoux, P. Chase, V. Gupta, T. Spicer, L. Scampavia, A. Singh, K.S. Carroll, First-in-class inhibitors of sulfur metabolism with bactericidal activity against non-replicating M. tuberculosis, ACS Chem. Biol. 11 (1) (2016) 172–184.
[19] B. Campanini, M. Pieroni, S. Raboni, S. Bettati, R. Benoni, C. Pecchini, G. Costantino, A. Mozzarelli, Inhibitors of the sulfur assimilation pathway in bacterial pathogens as enhancers of antibiotic therapy, Curr. Med. Chem. 22 (2) (2014) 187–213.
[20] Bhave DP, Muse III WB, Carroll KS. Drug Targets in Mycobacterial Sulfur Metabolism. Vol 7.; 2007.
[21] Kredich NM. Biosynthesis of Cysteine. Stewart V, ed. EcoSal Plus. 2008;3(1): ecosalplus.3.6.1.11. doi:10.1128/ecosalplus.3.6.1.11.
[22] Tyrrell R, Hg Verschueren K, Dodson EJ, Murshudov GN, Addy C, Wilkinson AJ. The Structure of the Cofactor-Binding Fragment of the LysR Family Member, CysB: A Familiar Fold with a Surprising Subunit Arrangement. http://biomednet.com/elecref/0969212600501017.
[23] B. Campanini, R. Benoni, S. Bettati, C.M. Beck, C.S. Hayes, A. Mozzarelli, Moonlighting O-acetylserine sulfhydrylase: New functions for an old protein, Biochim. Biophys. Acta - Proteins Proteomics. 1854 (9) (2015) 1184–1193, https://doi.org/10.1016/j.bbapap.2015.02.013.

[24] R. Benoni, O. De Bei, G. Paredi, C.S. Hayes, N. Franko, A. Mozzarelli, S. Bettati, B. Campanini, Modulation of Escherichia coli serine acetyltransferase catalytic activity in the cysteine synthase complex, FEBS Lett. 591 (9) (2017) 1212–1224.
[25] B. Campanini, F. Speroni, E. Salsi, P.F. Cook, S.L. Roderick, B. Huang, S. Bettati, A. Mozzarelli, Interaction of serine acetyltransferase with O -acetylserine sulfhydrylase active site: Evidence from fluorescence spectroscopy, Protein Sci. 14 (8) (2005) 2115–2124.
[26] B. Rosa, M. Marchetti, G. Paredi, H. Amenitsch, N. Franko, R. Benoni, B. Giabbai, M.G. De Marino, A. Mozzarelli, L. Ronda, P. Storici, B. Campanini, S. Bettati, Combination of SAXS and protein painting discloses the three-dimensional organization of the bacterial cysteine synthase complex, a potential target for enhancers of antibiotic action, Int. J. Mol. Sci. 20 (20) (2019) 5219.
[27] J. Huang, W. Song, H. Huang, Q. Sun, Pharmacological therapeutics targeting RNA-dependent RNA polymerase, proteinase and spike protein: From mechanistic studies to clinical trials for COVID-19, J. Clin. Med. 9 (4) (2020), https://doi.org/10.3390/jcm9041131.
[28] K. Mino, T. Yamanoue, T. Sakiyama, N. Eisaki, A. Matsuyama, K. Nakanishi, Effects of bienzyme complex formation of cysteine synthetase from escherichia coli on some properties andkinetics, Biosci. Biotechnol. Biochem. 64 (8) (2000) 1628–1640, https://doi.org/10.1271/bbb.64.1628.
[29] J. Magalhães, N. Franko, G. Annunziato, M. Welch, S.K. Dolan, A. Bruno, A. Mozzarelli, S. Armao, A. Jirgensons, M. Pieroni, G. Costantino, B. Campanini, Discovery of novel fragments inhibiting O-acetylserine sulphhydrylase by combining scaffold hopping and ligand–based drug design, J. Enzyme Inhib. Med. Chem. 33 (1) (2018) 1444–1452.
[30] J. Magalhães, N. Franko, G. Annunziato, M. Pieroni, R. Benoni, A. Nikitjuka, A. Mozzarelli, S. Bettati, A. Karawajczyk, A. Jirgensons, B. Campanini, G. Costantino, Refining the structure−activity relationships of 2-phenylcyclopropane carboxylic acids as inhibitors of O-acetylserine sulfhydrylase isoforms, J. Enzyme Inhib. Med. Chem. 34 (1) (2019) 31–43.
[31] J. Magalhães, G. Annunziato, N. Franko, M. Pieroni, B. Campanini, A. Bruno, G. Costantino, Integration of enhanced sampling methods with saturation transfer difference experiments to identify protein druggable pockets, J. Chem. Inf. Model. 58 (3) (2018) 710–723, https://doi.org/10.1021/acs.jcim.7b00733.
[32] M. Pieroni, G. Annunziato, C. Beato, R. Wouters, R. Benoni, B. Campanini, T. A. Pertinhez, S. Bettati, A. Mozzarelli, G. Costantino, Rational design, synthesis, and preliminary structure-activity relationships of α-substituted-2-phenylcyclopropane carboxylic acids as inhibitors of Salmonella typhimurium O-acetylserine sulfhydrylase, J. Med. Chem. 59 (6) (2016) 2567–2578, https://doi.org/10.1021/acs.jmedchem.5b01775.
[33] G. Annunziato, C. Spadini, N. Franko, P. Storici, N. Demitri, M. Pieroni, S. Flisi, L. Rosati, M. Iannarelli, M. Marchetti, J. Magalhaes, S. Bettati, A. Mozzarelli, C. S. Cabassi, B. Campanini, G. Costantino, Investigational studies on a hit compound cyclopropane-carboxylic acid derivative targeting O-acetylserine sulfhydrylase as a colistin adjuvant, ACS Infect. Diseases. 7 (2) (2021) 281–292, https://doi.org/10.1021/acsinfecdis.0c00378.
[34] S.M. Agarwal, R. Jain, A. Bhattacharya, A. Azam, Inhibitors of Escherichia coli serine acetyltransferase block proliferation of Entamoeba histolytica trophozoites, Int. J. Parasitol. 38 (2) (2008) 137–141, https://doi.org/10.1016/j.ijpara.2007.09.009.
[35] C. Chen, Q. Yan, M. Tao, H. Shi, X. Han, L. Jia, Y. Huang, L. Zhao, C. Wang, X. Ma, Y. Ma, Characterization of serine acetyltransferase (CysE) from methicillin-resistant Staphylococcus aureus and inhibitory effect of two natural products on CysE, Microb. Pathog. 131 (2019) 218–226.
[36] J. Magalhães, N. Franko, S. Raboni, G. Annunziato, P. Tammela, A. Bruno, S. Bettati, S. Armao, C. Spadini, C.S. Cabassi, A. Mozzarelli, M. Pieroni, B. Campanini, G. Costantino, Discovery of substituted (2-aminooxazol-4-yl) isoxazole-3- carboxylic acids as inhibitors of bacterial serine acetyltransferase in the quest for novel potential antibacterial adjuvants, Pharmaceuticals. 14 (2) (2021) 1–16, https://doi.org/10.3390/ph14020174.
[37] J. Magalhães, N. Franko, S. Raboni, G. Annunziato, P. Tammela, A. Bruno, S. Bettati, A. Mozzarelli, M. Pieroni, B. Campanini, G. Costantino, Inhibition of nonessential bacterial targets: discovery of a novel serine O-acetyltransferase inhibitor, ACS Med. Chem. Lett. 11 (5) (2020) 790–797, https://doi.org/10.1021/acsmedchemlett.9b00627.
[38] Chen W, Li K, Wang Y, Xi Z. Microwave-Assisted Synthesis of Benzothiazoleurea Derivatives.; 2010.
[39] K. Nepali, H.Y. Lee, J.P. Liou, Nitro-group-containing drugs, J. Med. Chem. 62 (6) (2019) 2851–2893, https://doi.org/10.1021/acs.jmedchem.8b00147.
[40] J. Bajorath, L. Peltason, M. Wawer, R. Guha, M.S. Lajiness, J.H. Van Drie, Navigating structure-activity landscapes, Drug Discov. Today 14 (13) (2009) 698–705, https://doi.org/10.1016/j.drudis.2009.04.003.
[41] L. Peltason, J. Bajorath, Molecular similarity analysis uncovers heterogeneous structure-activity relationships and variable activity landscapes, Chem. Biol. 14 (5) (2007) 489–497, https://doi.org/10.1016/j.chembiol.2007.03.011.
[42] T. Sander, J. Freyss, M. von Korff, C. Rufener, DataWarrior: An open-source program for chemistry aware data visualization and analysis, J. Chem. Inf. Model. 55 (2) (2015) 460–473, https://doi.org/10.1021/ci500588j.
[43] R. Guha, J.H. Van Drie, Structure−activity landscape index: identifying and quantifying activity cliffs, J. Chem. Inf. Model. 48 (3) (2008) 646–658, https://doi.org/10.1021/ci7004093.
[44] G.M. Maggiora, On outliers and activity cliffs why QSAR often disappoints, 1535-1535, J. Chem. Inf. Model. 46 (4) (2006), https://doi.org/10.1021/ci060117s.
[45] V.E. Pye, A.P. Tingey, R.L. Robson, P.C.E. Moody, The structure and mechanism of serine acetyltransferase from Escherichia Coli, J. Biol. Chem. 279 (39) (2004) 40729–40736, https://doi.org/10.1074/jbc.M403751200.
[46] Bank, R. P. D. RCSB PDB - 1T3D: Crystal structure of Serine Acetyltransferase from E.coli at 2.2A. https://www.rcsb.org/structure/1T3D (accessed 2022-06-20).
[47] O. Trott, A.J. Olson, AutoDock Vina: improving the speed and accuracy of docking with a new scoring function, efficient optimization, and multithreading, J. Comput. Chem. 31 (2) (2010) 455–461, https://doi.org/10.1002/jcc.21334.
[48] J. Eberhardt, D. Santos-Martins, A.F. Tillack, S. Forli, AutoDock Vina 1.2.0: New docking methods, expanded force field, and python bindings, J. Chem. Inf. Model. 61 (8) (2021) 3891–3898, https://doi.org/10.1021/acs.jcim.1c00203.
[49] C. Bergonzi, A. Di Natale, F. Zimetti, C. Marchi, A. Bianchera, F. Bernini, M. Silvestri, R. Bettini, L. Elviri, Study of 3D-printed chitosan scaffold features after different post-printing gelation processes, Sci. Rep. 9 (1) (2019), https://doi.org/10.1038/s41598-018-36613-8.